Toxicology Reports 2 (2015) 758–764

Contents lists available at ScienceDirect

Toxicology Reports

journal homepage: www.elsevier.com/locate/toxrep

The effects of silver nanoparticles on mouse embryonic stem cell self-renewal and proliferation

Pavan Rajanahalli[b], Christopher J. Stucke[c], Yiling Hong[a,*]

[a] College of Veterinary Medicine, Western University of Health Sciences, Pomona, CA 91766, USA
[b] College of Veterinary Medicine, Department of Anatomy and Physiology, Kansas State University, Manhattan, KA 66506, USA
[c] Kent State University College of Podiatric Medicine, 6000 Rockside Woods Boulevard Independence, OH 44131, USA

ARTICLE INFO

Article history:
Received 10 March 2015
Received in revised form 1 May 2015
Accepted 4 May 2015
Available online 16 May 2015

Keywords:
Silver nanoparticles (AgNPs)
Mouse embryonic stem cells (mESCs)
Self-renewal and proliferation
Nanotoxicity

ABSTRACT

Silver nanoparticles (AgNPs) are gaining rapid popularity in many commonly used medical and commercial products for their unique anti-bacterial properties. The molecular mechanisms of effects of AgNPs on stem cell self-renewal and proliferation have not yet been well understood. The aim of the work is to use mouse embryonic stem cells (mESCs) as a cellular model to evaluate the toxicity of AgNPs. mESC is a very special cell type which has self-renewal and differentiation properties. The objective of this project is to determine the effects of AgNPs with different surface chemical compositions on the self-renewal and cell cycle of mESCs. Two different surface chemical compositions of AgNPs, polysaccharide-coated and hydrocarbon-coated, were used to test their toxic effects on self-renewal and proliferation of mESCs. The results indicated that both polysaccharide-coated and hydrocarbon-coated AgNPs changed the cell morphology of mESCs. Cell cycle analysis indicated that AgNPs induced mESCs cell cycle arrest at G1 and S phases through inhibition of the hyperphosphorylation of Retinoblastoma (Rb) protein. Furthermore, AgNPs exposure reduced Oct4A isoform expression which is responsible for the pluripotency of mESCs, and induced the expression of several isoforms OCT4B-265, OCT4B-190, OCT4B-164 which were suggested involved in stem cell stresses responses. In addition, the evidence of reactive oxygen species (ROS) production with two different surface chemical compositions of AgNPs supported our hypothesis that the toxic effect AgNPs exposure is due to overproduction of ROS which altered the gene expression and protein modifications. Polysaccharide coating reduced ROS production, and thus reduced the AgNPs toxicity.

1. Introduction

Nanotechnology is a rapidly growing field with many uses in medicine and in the manufacture of commonly used products [1–3]. Among the hundreds of products that contain nanomaterials, the most widely used are AgNPs. AgNPs are most commonly used in medical and commercial products for their unique anti-bacterial properties and can be found in medical wound dressing, surgical instruments, and medical face masks to reduce microbial populations [4–6]. They are also used as filtering agents in humidifiers and water purification treatments [7].

AgNPs are highly chemically reactive due to their small size and high surface area, which produces a great amount of reactive oxygen species (ROS) [8]. ROS and free radical production cause oxidative stress, inflammation, and protein, DNA, and membrane damage. Studies on fibroblast cells have shown that AgNPs can enter human fibrosarcoma, skin carcinoma cells and primary neural cells and induce ROS and cell death while causing oxidative stress

* Corresponding author. Tel.: +1 909 469 8685.
E-mail address: yhong@westernu.edu (Y. Hong).

http://dx.doi.org/10.1016/j.toxrep.2015.05.005

and DNA damage [9–12]. Another study suggested that AgNPs induce cell death via up-regulation of p53-mediated apoptotic pathways [13]. AgNPs caused an increase in expression of p53, which is a tumor suppressor, p21, Noxa, Bax, and DNA damage repair proteins Rad 51 and H2AX [11,14,6,15].

The objective of this project is to determine the effects of AgNPs with and without coating on the self-renewal and cell cycle of mESCs. Polysaccharide-coated is the commonly employed coating/stabilizing agents for AgNPs applications. It has been shown that the coating will influence the particles shapes, sizes and surface properties will contribute to the AgNPs toxicity [16]. Many studies have shown toxic effects associated with nanoparticles introduced into a variety of human somatic cells and non-mammalian cells such as those of the zebrafish. However, little work has been done involving the effects that AgNPs have on embryonic stem cells [17]. Embryonic stem cells (ESCs) are clonal cell lines derived from the inner cell mass of a developing blastocyst [18,19]. They can proliferate indefinitely in vitro and also have the ability to differentiate into cells of all three germ layers (endoderm, mesoderm, and ectoderm), and thus ESCs is an excellent cellular model for classifying Engineered Nanoparticles (NPs) according to their toxic potential [19,20]. Our long-term objectives for the research are to understand the AgNPs toxic effects on self-renewal and proliferation of mouse mESCs and develop an Embryonic Stem Cell Test (EST) as a tool for classifying Engineered Nanoparticles (NPs) according to their toxic potential. We hypothesize that overproduction of ROS after AgNPs exposure can induce oxidative stress, which lead to alter key regulated genes expression and protein modification, and thus inhibition of cell renewal and cell growth. Furthermore, the proper AgNPs capping can reduce the toxicity by preventing the ROS production.

ESCs self-renewal properties and pluripotency characteristics are regulated by the interacting network of several transcription factors including Oct4 and Nanog. Oct4 is known as a master regulator and is exclusively found in ES cells. The OCT4 gene can generate at least two transcripts (OCT4A, OCT4B) by alternative splicing [21,22]. OCT4A is the most commonly described transcript, which is translated into a full-length nuclear-localized OCT4 protein with N- and C-terminal transactivation domains separated by a POU DNA-binding domain. This transcript is a transcription factor responsible for the pluripotency of ESCs. In contrast, the Oct4B transcript is truncated without exon 1. Because Oct4B cannot sustain ES cell self-renewal, it was suggested that it may be responsible to cellular stresses. Furthermore, a single OCT4B transcript may encode at least three protein isoforms, OCT4B-265, OCT4B-190 and OCT4B-164, by alternative translation through an internal site of OCT4B mRNA [23]. However, the function of Oct4B and how its alternative translation is regulated are unclear. Our results provided the evidence to support the function of Oct4B in stem cell stress response.

The cell cycle regulation is monitored by a cell cycle control system that responds to various intracellular and extracellular signals. If a cell is under stress, the control system will shut down the cell cycle at one of its several checkpoints [21]. We have examined the expression of Retinoblastoma (Rb) which is a critical protein plays a protective role in response to genotoxic stress by inhibiting the cell cycle at the G_1/S checkpoint. Hyperphosphorylation of Rb inactivates the protein which allows the E2F transcription factor to detach and push the cells into the S phase of the cell cycle. If Rb is hypophosphorylated or not phosphorylated at all, it is active and remains attached to the E2F transcription factor, causing cell cycle arrest. Studying the protein modification in response to AgNPs treatment will offer better understanding of the molecular mechanisms of nanotoxicity and provide the biomarkers for nanotoxicity analysis.

2. Materials and methods

2.1. Characterization of silver nanoparticles (AgNPs)

The two types of AgNPs used in this study differed primarily in their surface chemical composition. The 20 nm hydrocarbon-coated AgNPs were processed with hydrocarbons that prevent sintering, but leave a non-uniform hydrocarbon surface layer. Polysaccharide-coated AgNPs were a generous gift from Dr. Dan Goia (Clarkson University, Center for Advanced Materials Processing, Potsdam, NY). The 20 nm polysaccharide-coated AgNPs were synthesized with surface capping using a polysaccharide (acacia gum). The sizes of AgNPs in the solution were characterized using transmission electron microscopy (TEM) on a Hitachi H-7600 tungsten-tip instrument at an accelerating voltage of 100 kV. The AgNPs were suspended in deionized water at 1 mg/ml and then sonicated using a Branson-1510 sonicator bath at room temperature for 15 min at 35–40 W to aid in mixing and forming a homogeneous dispersion. For size measurements, sonicated 1 mg/ml AgNPs stock solution was diluted to a 50 μg/ml working solution. AgNPs were examined after NPs suspensions were deposited in carbon film-coated Cu grids. The advance microscopy techniques (AMT) software for the digital TEM camera was calibrated for size measurements of the nanoparticles. Information on mean size and SD was calculated using the point-to-point method as described elsewhere [25]. The result showed that the size of the majority AgNPs are between 5.0 and 20 nm (Supplementary Fig. 1a and b). Polysaccharide-coated nanoparticles tend to be individually distributed, whereas hydrocarbon-coated particles tend to agglomerate.

Supplementary material related to this article can be found, in the online version, at doi:10.1016/j.toxrep.2015.05.005.

2.2. mESCs cell culture and AgNPs treatments

J11 mESCs cells were a gift from Dr. Peter Stambrook (College of Medicine, University of Cincinnati). The cells were cultured on DMEM supplemented with 5% penicillin-streptomycin, 1X non-essential amino acids (NEAA, GIBCO Cat # 11140) and 1X Glutamax (GIBCO Cat # 35050), 10% embryonic stem cell qualified FBS (USA Scientific Cat # 98375200), 0.1 μM β-mercaptoethanol (Sigma Cat # M6250) and 50 μM leukemia inhibitory factor (LIF, Millipore Cat # ESG 1107). AgNPs solutions were prepared

in cell culture media (Ham's F12/DMEM) without serum prior to each experiment. The solutions were sonicated at room temperature for 30 min at 40 W to prevent AgNPs from agglomerating. Specific concentrations of AgNPs (5 and 50 μg/ml) were added to mESCs (60% confluence) and images were captured prior to harvesting cells at 24, 48 and 72 h for further analysis.

2.3. Reactive oxygen species (ROS) assay

Treated and untreated mESCs were incubated with 5 μM CellROX Deep Red Reagent (GIBCO, Cat # C10422) for 30 min in the dark at 37 °C and 10% CO_2 in mESC cell culture media and washed 3X in PBS (pH 7.2–7.6). CellROX Deep Red Reagent is a cell-permanent dye with absorption/emission maxima of ~644/665 nm. Images were taken by a confocal microscope (Olympus, Cy5 channel) accompanied with Fluoview image acquisition and analysis software.

2.4. Western blotting

Harvested cells of control and treated mESCs cell pellets were lysed with 100 μl RIPA buffer (Tris–HCl-pH 7.4:50 mM, NP-40: 1%, Sodium deoxycholate: 0.25%, NaCl: 150 mM, EDTA: 1 mM). The lysates were centrifuged at $1000 \times g$ for 1 min and 100 μl of 2X loading dye was added to 100 μl of cell lysates. A sodium dodecyl sulfate polyacrylamide gel electrophoresis (8%, SDS-PAGE) was performed to separate the proteins in the samples, and then transferred to a polyvinylidine difluoride (PVDF, Millipore) membrane. The membrane was probed with Oct-4 (Santa Cruz, Cat # SC-5279) and Rb (Santa Cruz, Cat # SC-74570) primary antibodies overnight at 4 °C, followed by incubation in respective secondary antibodies for 1 h at room temperature. Bands were visualized using chemiluminescent techniques with non-saturating exposures using X-ray films. Anti-β-actin antibody was used as a loading control for all the antibodies as mentioned above.

2.5. Flow cytometry

mESCs were treated for 24 and 48 h with both 5 and 50 μg/ml, polysaccharide-coated and hydrocarbon-coated AgNPs. The EZ-BrdU cell proliferation kit (Phoenix Flow Systems, Cat # AC1101) was used to determine changes in cell cycle phases in control and treated mESCs. BrdU Photolyte was added in AgNPs treated mESCs for 24 h and each time-point was examined followed by further experimental procedure according to the manufacturer's protocol. After BrdU treatment, cells were harvested using 0.25% trypsin and centrifuged for 5 min. The supernatant was aspirated and the pellet was gently resuspended with wash buffer and centrifuged. The pellet was re-suspended in 70% (v/v) ice cold ethanol (cell density was adjusted to $1–2 \times 10^6$ cells/ml) and stored at least overnight or until ready to use at −20 °C. Finally, the pellet was washed with 2 ml of rinse buffer, centrifuged. An appropriate amount of fluorescein-PRB1 (5 μl of anti-BrdU and 95 μl of rinse buffer for each assay) was added to the cell pellet, resuspended and incubated for 60 min in the dark at room temperature. 500 μl of PI/RNase A solution was added and incubated for 30 min in the dark at room temperature. The cells were analyzed within 3 h of staining using a BD FACS Calibur Flow Cytometer (BD FACS Calibur™) with FlowJo (version 9) software. The cells were excited at 488 nm and appropriate filters were used to capture BrdU-FITC and PI positive signals in separate channels. Data analysis was performed using ModFit LT 3.1 and Cell Quest Pro software.

3. Results

3.1. AgNPs altered mESCs colony morphology

Two different surface chemical compositions of AgNPs, polysaccharide-coated and hydrocarbon-coated, were used to test their effects on mESCs self-renewal and cell proliferation. When the mESCs were exposed to both polysaccharide and hydrocarbon-coated AgNPs at concentrations of 5 and 50 μg/ml, the colonies showed an irregular morphology with flat and rough edges even at low concentration (5 μg/ml). These morphologies are atypical for normal mESCs colonies. Furthermore, many colonies started to disassociate and become single floating cells 24 h after the treatment (Fig. 1a). The polysaccharide-coated AgNPs treatment had a lower single cell population compared to hydrocarbon-coated AgNPs indicating that the polysaccharide coating had reduced toxicity to mESCs (Fig. 1b).

3.2. AgNPs increased ROS production in mESCs

In order to investigate the cause of the stress by AgNPs, mESCs were exposed to 5 and 50 μg/ml polysaccharide-coated AgNPs and hydrocarbon-coated AgNPs. The CellROX® Deep Red reagent was used to compare the ROS production levels in each treatment. The dye showed non-fluorescence while in a reduced state and became fluorescent upon oxidation by reactive oxygen species with an emission maxima of ~665 nm that can be measurable by fluorescent imaging. When the cells were exposed to AgNPs, the fluorescence intensity increased, which indicated that ROS production increased. As shown in Fig. 2aand c, the red fluorescence intensity was increased within 24 h in mESCs as the concentration increased from 5 μg/ml to 50 μg/ml after the polysaccharide-coated AgNPs treatment. On the other hand, hydrocarbon-coated AgNPs produced a stronger red fluorescent signal than the polysaccharide-coated at 5 μg/ml concentration treatment, but the fluorescent signal was weaker at the 50 μg/ml treatment because cell death was occurring at that concentration hydrocarbon-coated AgNPs treatment (Fig. 2b and d). The results indicated that the polysaccharide-coated reduced the ROS production.

3.3. AgNPs induced mESCs cell cycle arrest through preventing phosphorylation of Retinoblastoma (Rb)

The cell cycle analysis study indicated that AgNPs drastically alter mESCs cell cycle distributions (Fig. 3a and b). 24 h after the hydrocarbon-coated AgNPs treatment (5 μg/ml),

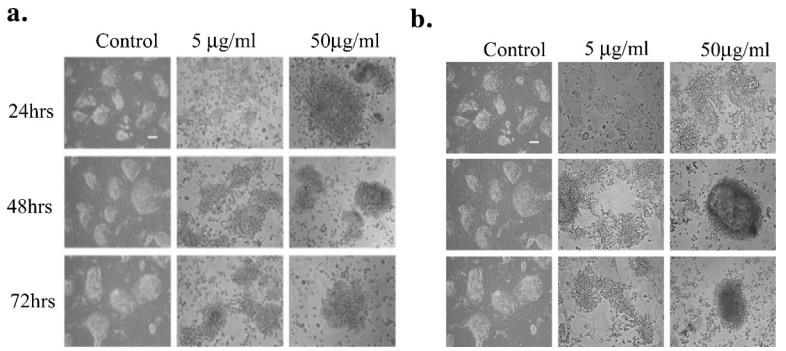

Fig. 1. AgNPs disrupted normal stem cell colony morphology. (a). Phase contrast images of mESC treated with 5 and 50 μg/ml hydrocarbon-coated AgNPs. The cells were exposed to AgNPs for 24, 48 and 72 h. (b). Phase contrast images of mESCs treated with 5 and 50 μg/ml polysaccharide-coated AgNPs. Images were acquired by an inverted microscope (Nikon TS100) at 10× magnification using MetaMorph Imaging Software.

43.69% of the mES cells were in G1 phase, 0.00% were in S phase, and 56.31% were in G2 phase compared to the untreated control cells consisting of 23.19% of the cells in G1 phase, 59.73% in S phase, and 17.08% in G2 phase. 48 h later, most of the cells were arrested in S phase (82%). 16.3% of cells were in G1 phase, and only 1.15% were in G2 phase. The cell cycle distribution of polysaccharide-coated AgNPs treated cells (5 μg/ml) followed a similar trend as hydrocarbon-coated nanoparticles showed no S phase activity (0.00%) and a higher percentage of cells in G1 (45.1%) and G2 (54.9%) 24 h after the treatment. 48 h after the treatment, most of the cells were arrested in S phase (79.54%), 19.31% of cells in G1 phase, and only 1.15% in G2 phase. Together these results indicated that both AgNPs induced cell cycle arrest in at the G1 checkpoint in the first 24 h of treatment, and most of cells were arrested in the S phase 48 h after the treatment (Fig. 3c and d). To provide an insight into the molecular mechanisms of the effect of AgNPs on cell cycle progression in mESCs, the status of Rb protein phosphorylation were examined via western blotting. The results showed that both AgNPs eliminated the hyperphosphorylation of Rb compared with untreated cells mESCs at 5 μg/ml (Fig. 4a and b). Dephosphorylation of Rb protein allowed Rb to bind to the E2F transcription

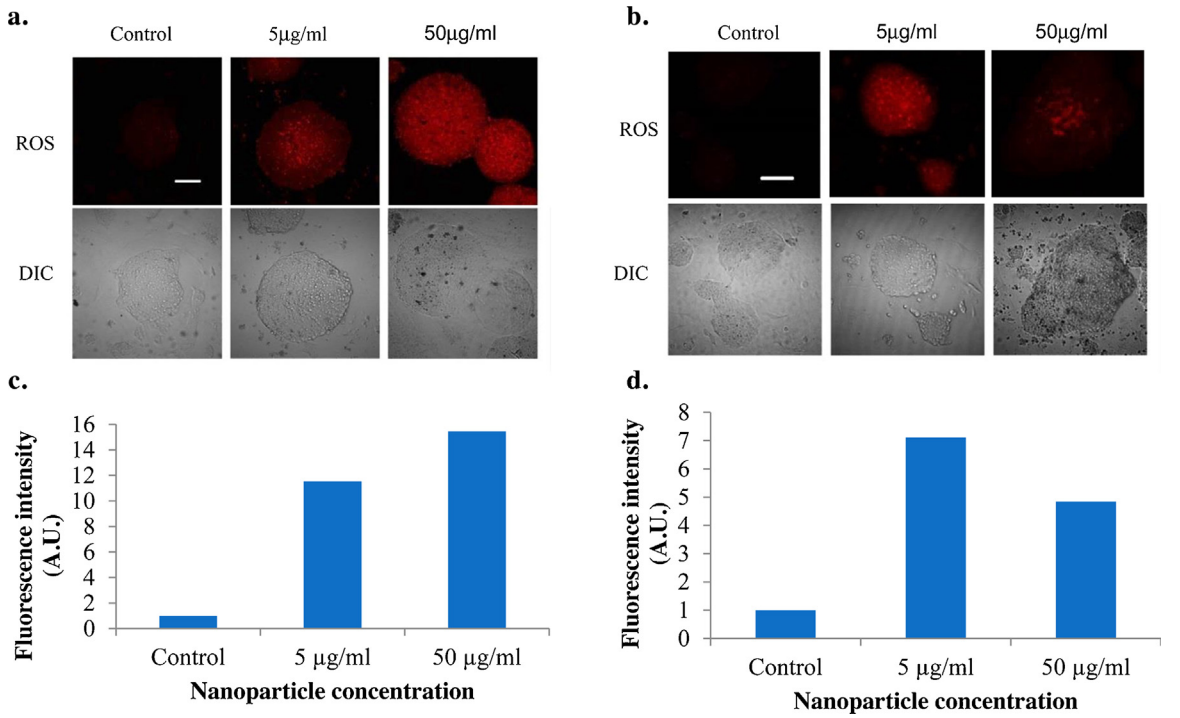

Fig. 2. ROS production increased in mESCs after exposure to AgNPs. (a). mESCs were treated with 5 μg/ml and 50 μg/ml concentrations of polysaccharide-coated AgNPs for 24 h. The left panel is untreated control cells. The red fluorescence increased as the concentration of AgNPs increased. (b). The cells treated with hydrocarbon-coated AgNPs for 24 h. The red fluorescence signifies the presence of ROS at 5 μg/ml treatment. The reduced red fluorescence at 50 μg/ml of hydrocarbon-coated AgNPs might be due to cell death occurring at this dose of treatment. (c). The mESCs red fluorescence intensity treated with 5 μg/ml and 50 μg/ml concentrations of polysaccharide-coated AgNPs for 24 h was quantitated with image J software. (d). The mESCs red fluorescence intensity treated with 5 μg/ml and 50 μg/ml concentrations of hydrocarbon-coated AgNPs for 24 h was quantitated with image J software.

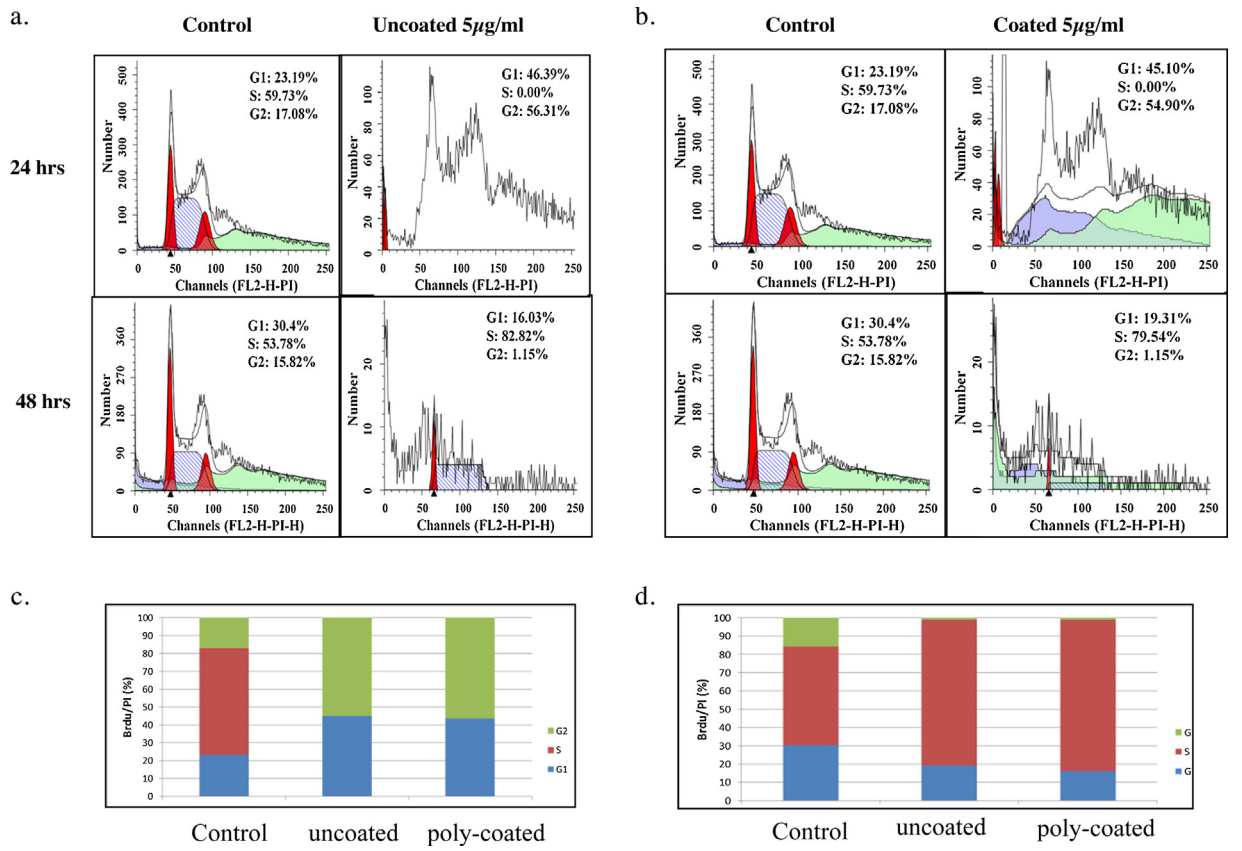

Fig. 3. AgNPs promoted cell cycle arrest at G1/S checkpoint in mESCs. (a). mESCs were treated with polysaccharide-coated AgNPs at 5 μg/ml and 50 μg/ml for 24, 48, and 72 h. The cells were analyzed by flow cytometry, which plots the cell count versus DNA content. (b). mES cells were treated with hydrocarbon-coated at 5 μg/ml and 50 μg/ml. (c). Graphic bars indicated at 24 h treatment most of cells are in G1 and G2 phase. (d). Graphic bars indicated that most of the cells are in the S phase at 48 h after treatment.

factor, stopping the cell cycle progress. The dephosphorylation of Rb correlated with cell cycle studies showing G1/S arrest within 24 h. Furthermore, there was also evidence of increasing 5 kDa Rb cleavage band at 5 μg/ml after longer incubation. Previous research had suggested this cleavage is associated with apoptosis [24]. The Rb level is very low at 50 μg/ml hydrocarbon-coated AgNPs treatment due to the cell death. The result of β-actin loading control indicated that we lose a lot of cells at that dose of treatment.

3.4. AgNPs altered OCT4 gene expression

Oct4 is well known as a master regulator in maintaining ES self-renewal and differentiation. Oct4 levels

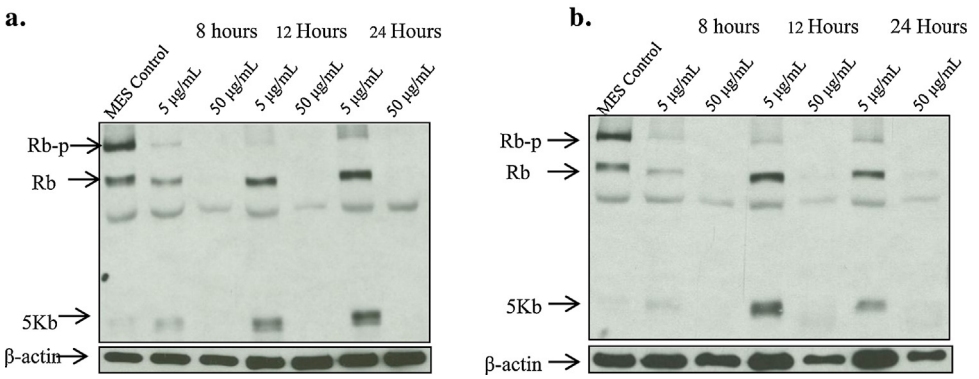

Fig. 4. AgNPs induced Rb dephosphorylation and cleavage of a 5 kDa fragment in mESCs. (a). mESCs treated with 5 μg/ml and 50 μ/ml of polysaccharide-coated AgNPs for 8, 12, 24 h. The cell extracts were subjected to western blotting and probed with Rb monoclonal antibody. The upper band shows hyperphosphorylation and the lower band indicated the cleavage of a 5 kDa fragment. (b). mESCs treated with 5 μg/ml and 50 μ/ml of hydrocarbon-coated AgNPs for 8, 12, 24 h. The cell extracts were subjected to western blotting and probed with Rb monoclonal antibody. β-actin was used as a loading control.

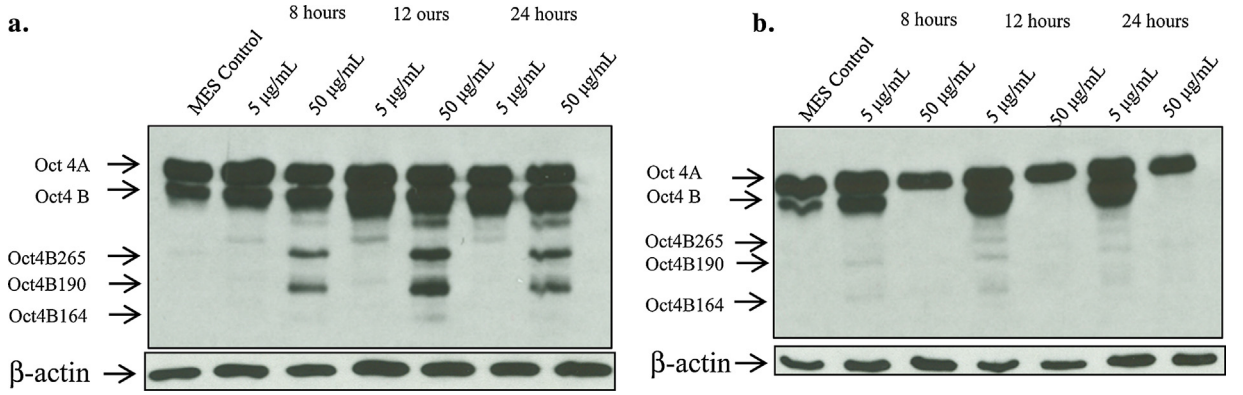

Fig. 5. AgNP induced changes OCT4 gene expression. (a). mESCs treated with 5 μg/ml and 50 μg/ml of polysaccharide-coated AgNPs for 8, 12, and 24 h were analyzed via western blotting with Oct-4 antibody. Within 8 h the AgNP induced the Oct4B isoform expression. (b). mESCs treated with 5 μg/ml and 50 μg/ml of hydrocarbon-coated AgNPs for 8, 12, and 24 h. Oct4B isoforms were induced in the 5 μg/ml treatment but not in the 50 μg/ml treatments. β-actin as a loading control.

must be tightly regulated in order to maintain pluripotency of ESCs. The OCT4 gene can generate at least two transcripts (OCT4A, OCT4B) by alternative splicing. OCT4A is a transcription factor responsible for the pluripotency of ESCs. In contrast, the Oct4B transcript is truncated without exon 1. Because Oct4B cannot sustain ESCs cell self-renewal, it was suggested that it may be responsible to cellular stresses [23]. To study whether OCT4 expression was affected by the AgNPs exposure, Oct4 protein expression was analyzed by western blotting. Fig. 5 demonstrated that the protein level of Oct4A was reduced and Oct4B was increased. Furthermore, there were multiple smaller bands with the molecule weight about OCT4B-265, OCT4B-190, OCT4B-164 appeared in response to AgNPs treatments. This data provided the evidence that AgNPs induced the Oct4B isoforms OCT4B-265, OCT4B-190, OCT4B-164 expression. The lower density isoforms that were seen in hydrocarbon-coated treatment was due to more cells underwent apoptosis. Further study of the correlation of the expression of Oct4B protein expression with different AgNPs coating will provide important insights on the mechanism of nanotoxicity and role of OCT4 gene in stem cell stress response.

4. Discussion

AgNPs are highly reactive toward biomolecules due to their high surface area to weight ratio, which makes them very versatile for use in consumer products and medical equipment. Their wide range of application causes them to be highly exposed to humans and the environment. Our results show that the AgNPs treatments caused increased ROS levels and counteracted the effects on mESCs self-renewal and proliferation. The results obtained from the Rb phosphorylation supported the claim of cell cycle arrest at the G_1/S transition because it experienced a decrease in hyperphosphorylation of Rb protein. This study provided an insight into the molecular mechanisms of the effect of AgNPs on stem cell self-renewal and cell cycle progression. Furthermore, there was also evidence of a 5 kDa Rb cleavage band, which previous research has suggested is associated with apoptosis [24]. Further study associated with this cleavage will need to pursue. In addition, to better understand the molecular mechanism of impact of AgNPs on stem cell self-renewal, we examine the Oct4 protein expression in response to AgNPs treatment. The result indicated that when mESCs were exposed to AgNPs for 8 h, Oct4B-265, OCT4B-190 and OCT4B-164 were induced. Similar isoforms were seen within 4 h after exposure to ionizing radiation (data not shown). The isoforms has been suggested via alternative translation and alternative splicing [21]. Alternative translation offers an additional layer of complexity and regulation in protein production, creating protein variants that may differ in function and localization. Our data suggested that OCT4 gene not only plays an important role in stem cell self-renewal, but it also has a very important role in maintaining the stem cell's genomic stability and cell fate through alternative splicing and translation. In response to the stress, alternative splicing and translation produces Oct4B and its variants to prevent stem cell renewal and undertake a program of repair or cell death. Further investigations are needed to test this hypothesis by identifying the factors involved in regulating the alternative splicing and translational regulation and studying the role of each isoform of Oct4 in response to the stress. The studies will lead to a better understanding of the role of Oct4 and the molecular mechanisms of how a stem cell responds to stress. It will also provide necessary scientific data for potential toxicity of nanoparticles.

In conclusion, our study demonstrates that AgNPs can induce cell cycle arrest, alter cell cycle checkpoint protein expression and prevent stem cell self-renewal. We hypothesize that AgNPs induced ROS production, which lead cells failing to maintain normal physiological redox-regulated functions. This can lead to change gene expression and protein modification. Based on this hypothesis, modification of the surface chemistry of AgNPs could reduce the ROS production and thus alter the toxicity of these NPs. Our study found that polysaccharide-coated nanoparticles were less toxic because they tend to be individually distributed, and produce less ROS, whereas hydrocarbon-coated particles

tend to agglomerate. Overall, across most of our studies, it appeared that hydrocarbon-coated AgNPs treatments produced greater toxic effects than polysaccharide-coated treatments. This is could be due to the polysaccharide coating interfering with interactions between the AgNPs and water, reducing ROS production. Further detailed studies on the mechanisms of differential aggregation or dissolution effects of these particles are needed to better understand the relationship of the surface chemistry of the nanoparticles and their toxicity effects.

Conflict of interest

None declared.

Acknowledgments

This work was supported by National Institutes of Environmental Health Sciences (1R15 ES019298-01A1).

The hydrocarbons-coated AgNPs was a kind gift donated by Dr. Karl Martin (Novacentrix, Austin, TX, formerly Nanotechnologies, Inc.)

Polysaccharide-coated AgNPs was a kind gift donated by Dr. Dan Goia (Clarkson University, Center for Advanced Materials Processing, Potsdam, NY).

References

[1] M. Bruchez, M. Moronne, P. Gin, S. Weiss, A.P. Alivisatos, Semiconductor nanocrystals as fluorescent biological labels, Science 281 (1998) 2013–2016.
[2] J. West, N. Halas, Applications of nanotechnology to biotechnology, Curr. Opin. Biotechnol. 11 (2000) 215–217.
[3] E.C. Wang, A.Z. Wang, Nanoparticles and their applications in cell and molecular biology, Integr. Biol. 6 (2014) 9–26.
[4] V. Colvin, The potential environmental impacts of engineered nanomaterials, Nat. Biotechnol. 21 (2003) 1166–1170.
[5] C.F. Chau, S.H. Wu, G.C. Yen, The development of regulations for food nanotechnology, Trends Food Sci. Technol. 18 (2007) 269–280.
[6] M. Ahamed, M.S. Alsalhi, M.K. Siddiqui, Silver nanoparticle applications and human health, Clin. Chim. Acta 411 (2010) 1841–1848.
[7] S.M. Hussain, J. Schlager, Safety evaluation of silver nanoparticles: inhalation model for chronic exposure, Oxf. J. 108 (2009) 223–224.
[8] R. Foldbjerg, P. Olesen, M. Hougaard, D.A. Dang, H.J. Hoffmann, H. Autrup, PVP-coated silver nanoparticles and silver ions induce reactive oxygen species, apoptosis and necrosis in THP-1 monocytes, Toxicol. Lett. 190 (2) (2009) 156–162.
[9] S. Arora, J. Jain, J.M. Rajwade, K.M. Paknikar, Cellular responses induced by silver nanoparticles: in vitro studies, Toxicol. Lett. 179 (2008) 93–100.
[10] S. Arora, J. Jain, J.M. Rajwade, K.M. Paknikar, Interactions of silver nanoparticles with primary mouse fibroblasts and liver cells, Toxicol. Appl. Pharmacol. 236 (2009) 310–318.
[11] L. Zhu, C. Wook, L. Dai, Y. Hong, DNA damage induced by multiwalled carbon nanotubes in mouse embryonic stem cells, Nano Lett. 7 (2007), 3592–3579.
[12] A. Haase, S. Rott, A. Mantion, P. Graf, J. Plendl, A.F. Thunemann, W.P. Meier, A. Taubert, A. Luch, G. Reiser, Effects of silver nanoparticles on primary mixed neural cell cultures: uptake, oxidative stress and acute calcium responses, Toxicol. Sci. 126 (2) (2012) 457–468.
[13] P. Gopinath, S.K. Gogoi, P. Sanpuic, A. Paul, A. Chattopadhyay, S.S. Ghosh, Signaling gene cascade in silver nanoparticle induced apoptosis, Colloids Surf. B: Biointerfaces 77 (2010) 240–245.
[14] M. Ahamed, M. Karns, M. Goodson, J. Rowe, S. Hussain, J. Schlager, Y. Hong, DNA damage responses to different surface chemistry of silver nanoparticles in mammalian cells, Toxicol. Appl. Pharmacol. 233 (2008) 404–410.
[15] K. Meyer, P. Rajanahalli, M. Ahamed, J. Rowe, Y. Hong, ZnO nanoparticles induce apoptosis in human dermal fibroblast cells via P53 and p38 pathway, Toxicol. In Vitro 25 (2011) 1721–1726.
[16] L.K. Braydich-Stolle, E.K. Breitner, K.K. Comfort, J.J. Schlager, S.M. SHussain, Dynamic characteristics of silver nanoparticles in physiological fluids: toxicological implications, Langmuir 30 (50) (2014) 15309–15316.
[17] L.K. Braydich-Stolle, B. Lucas, A. Schrand, R.C. Murdock, T. Lee, J.J. Schlager, S.M. Hussain, M.C. Hofmann, Silver nanoparticles disrupt GDNF/Fyn kinase signaling in spermatogonial stem cells, Toxicol. Sci. 116 (2) (2010) 577–589.
[18] J.A. Thomson, Embryonic stem cell lines derived from human blastocysts, Science 282 (1998) 1145–1147.
[19] E.S. Wong, K.H. Ban, R. Mutalif, N.A. Jenkins, N.G. Copeland, C.L. Stewart, A simple procedure for the efficient derivation of mouse ES cells, Methods Enzymol. 476 (2010) 265–283.
[20] J.S. Odorico, D.S. Kaufman, J.A. Thomson, Multilineage differentiation from human embryonic stem cells lines, Stem Cells 19 (2001) 193–204.
[21] X. Wang, Y. Zhao, Z. Xiao, B. Chen, Z. Wei, B. Bin Wang, J. Zhang, J. Han, Y. Gao, L. Li, H. Zhao, W. Zhao, H. Lin, J. Dai, Alternative translation of OCT4 by an internal ribosome entry site and its novel function in stress response, Stem Cells 27 (2009) 1265–1275.
[22] N. Salomonis, C.R. Schlieve, L. Pereira, et al., Alternative splicing regulates mouse embryonic stem cell pluripotency and differentiation, Proc. Natl. Acad. Sci. U. S. A. 107 (2010) 10514–10519.
[23] Y. Gao, X. Wang, J. Han, Z. Xiao, B. Chen, G. Su, J. Dai, The novel OCT4 spliced variant OCT4B1 can generate three protein isoforms by alternative splicing into OCT4B, J. Genet. Genomics 37 (7) (2010) 461–465.
[24] W. Chen, G. Otterson, S. Lipkowitz, S. Khleif, A. Coxon, F. Kaye, Apoptosis is associated with cleavage of a 5 kDa fragment from RB which mimics dephosphorylation and modulates E2F binding, Oncogene 14 (1997) 1243–1248.
[25] R.C. Murdock, L. Braydich-Stolle, A.M. Schrand, J.J. Schlager, S.M. Hussain, Characterization of nanomaterial dispersion in solution prior to invitro exposure using dynamic light scattering technique, Toxicol. Sci. 101 (2008) 239–253.